Metal-Organic Frameworks

International Edition: DOI: 10.1002/anie.201505461
German Edition: DOI: 10.1002/ange.201505461

Definitive Molecular Level Characterization of Defects in UiO-66 Crystals

*Christopher A. Trickett, Kevin J. Gagnon, Seungkyu Lee, Felipe Gándara, Hans-Beat Bürgi, and Omar M. Yaghi**

Abstract: *The identification and characterization of defects, on the molecular level, in metal-organic frameworks (MOFs) remain a challenge. With the extensive use of single-crystal X-ray diffraction (SXRD), the missing linker defects in the zirconium-based MOF UiO-66, $Zr_6O_4(OH)_4(C_8H_4O_4)_6$, have been identified as water molecules coordinated directly to the zirconium centers. Charge balancing is achieved by hydroxide anions, which are hydrogen bonded within the pores of the framework. Furthermore, the precise nature of the defects and their concentration can be manipulated by altering the starting materials, synthesis conditions, and post-synthetic modifications.*

Structural defects in solids have a well-established role in enhancing and controlling the properties of materials, most notably in heterogeneous catalysis and band-gap tuning of semiconductors.[1–5] The characterization of such defects has involved a combination of techniques such as electron[6] and fluorescence microscopy,[7] Raman,[8] infrared,[9] and X-ray photoelectron spectroscopy,[10] powder X-ray diffraction combined with density functional theory calculations,[11] and single-crystal X-ray diffraction (SXRD).[12,13] Metal-organic frameworks (MOFs) in which metal oxide hubs are joined by organic linkers to make porous structures are increasingly found to have defective structures by virtue of missing linkers.[14–17] For example, three MOF structures, MOF-5, HKUST-1, and UiO-66, have been identified to contain defect sites.[7,10,18,19] However, in both the established inorganic solids mentioned above and MOFs, the molecular level determination of the nature of these sites is not easily elucidated because of the ambiguities associated with deciphering low concentrations of electron density. The porous nature of MOFs allows chemical modification of defect sites without changing the underlying connectivity of the overall structure, and thus provides definitive means of achieving the molecular-level characterization of defects.

Herein, we show for the first time how the precise structure of defects in MOFs can be determined from SXRD data. We use as an illustrative example the zirconium-based MOF called UiO-66 [$Zr_6O_4(OH)_4(C_8H_4O_4)_6$], first reported in 2008,[20] whose structure is found to readily crystallize with missing organic linker defects. There have been numerous studies using neutron[21] and X-ray powder diffraction, extended X-ray absorption fine structure,[22] and, in one case, SXRD[23] to characterize the nature of the defective sites. Thus far, a molecular level characterization of the defects and their precise structure and composition remain a challenge. Gaining such knowledge is imperative in light of the utility of this MOF in catalysis, adsorption, and its thermally and chemically robust structure.[24] This importance is underlined by the large number of studies (287 papers on UiO-66 from 2008 to 2014) focused on its chemistry.

The structure consists of an octahedron of zirconium atoms whose faces are capped by μ^3-oxo and μ^3-hydroxy groups in an alternating fashion. The octahedral edges are bridged by carboxylate groups from the benzenedicarboxylate (BDC) linker (Figure 1). UiO-66 has been shown from powder neutron diffraction[21] and later SXRD[23] to contain defect sites. Depending on the synthesis conditions employed, a significant portion of the BDC linkers are replaced by another species. The identity of the defects has been the subject of extensive scrutiny, with contradictory reports postulating the species replacing the linker to be water, hydroxide,[22,26] chloride,[27] modulators such as formate and acetate,[21] or solvent molecules such as *N*,*N*-dimethylformamide.[22] Additionally, it was recently found that under certain synthesis conditions, primitive nanodomains form within hafnium-based UiO-66, likely related to the defects.[11] Besides the uncertainty of the molecular identity of these defects, there has been no indication of what causes the relatively large percentage of missing linkers in an otherwise highly crystalline material.

A significant limitation in conclusively identifying the defect species has been the microcrystalline nature of UiO-66, with the largest crystals reaching only 10 μm.[23] We report the

[*] C. A. Trickett, S. Lee, Prof. O. M. Yaghi
Department of Chemistry, University of California-Berkeley
Materials Sciences Division, Lawrence Berkeley National Laboratory
Kavli Energy Nanosciences Institute at Berkeley
Center for Global Science at Berkeley
Berkeley, CA 94720 (USA)
E-mail: yaghi@berkeley.edu
Dr. K. J. Gagnon
Advanced Light Source, Lawrence Berkeley National Laboratory
Berkeley, CA 94720 (USA)
Dr. F. Gándara
Department of New Architectures in Materials Chemistry, Materials Science Institute of Madrid, Consejo Superior de Investigaciones Científicas
Madrid 28049 (Spain)
Prof. H.-B. Bürgi
Visiting Scholar at University of California – Berkeley
Institute of Chemistry, University of Zürich
Winterthurestrasse, 190, 8057 Zürich (Switzerland)
Prof. O. M. Yaghi
King Abdulaziz City of Science and Technology
P.O. Box 6086, Riyadh 11442 (Saudi Arabia)

Supporting information for this article is available on the WWW under http://dx.doi.org/10.1002/anie.201505461.

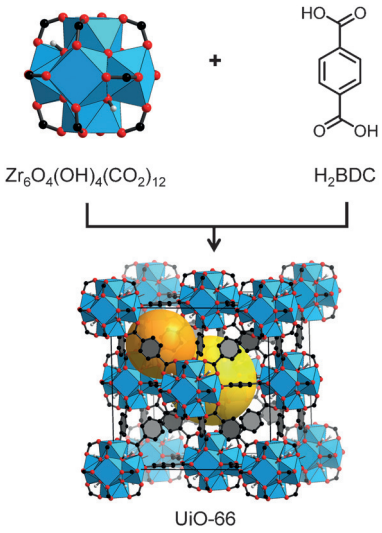

Figure 1. The defect-free SXRD structure of UiO-66 with 12-coordinated Zr-based metal clusters interconnected by benzenedicarboxylate (BDC) linkers in a face-centered cubic array. Atom labeling scheme: C, black; O, red; Zr, blue polyhedra; H, white; tetrahedral cavity, orange; octahedral cavity, yellow. Hydrogen atoms on the BDC link have been omitted for clarity.

identity and postulate the origin of the defects in the structure, of which the former is consistent across all synthesis conditions studied. This was facilitated by our development of a highly versatile synthesis of large single crystals up to 300 μm in diameter (Figure 2) that can be achieved from

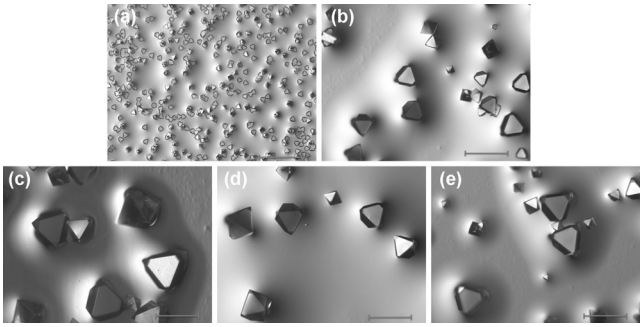

Figure 2. Optical microscope images of typical UiO-66 crystals synthesized from varying the ratio of formic acid to DEF: a) 0.5:1 formic acid/DEF; b) 0.75:1; c) 1:1; d) 1.25:1; e) 2:1. The crystal size reaches a maximum at a 1:1 ratio of DEF/formic acid. Scale bar on each image is 300 μm.

a variety of zirconium salts and functionalized linkers. In this study we postulate the origin of the defects in the structure and identify the species at the defect site as a water molecule, with the charge balance achieved by a hydroxide counterion located at hydrogen-bonding distance to the μ^3-OH group on the cluster. In some cases there is also an excess of oxide over hydroxide in the metal-oxide cluster.

Since the starting salt, $ZrOCl_2{\cdot}8H_2O$, in reality consists of rings of four eight-coordinated zirconium atoms, with bridging hydroxide groups and terminal water molecules, the charge in this salt is compensated by hydrogen-bonded chloride counterions.[28] Combined with experimental evidence for the water and hydroxide species in UiO-66, we hypothesize that both the counterion species and the coordinated water must be displaced during the synthesis by the negatively charged BDC linker to maintain charge neutrality, yet not all species are displaced by BDC prior to the crystallization of the structure.

The asymmetric unit of UiO-66 synthesized from zirconium oxychloride octahydrate is shown in Figure 3. In the

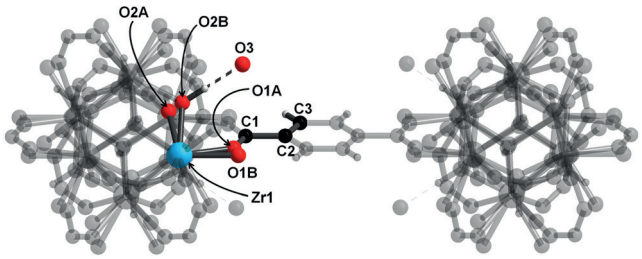

Figure 3. The asymmetric unit of UiO-66 is highlighted in color with Zr, blue; O, red; C, black; H, white.

following discussion, the atom at the defect site will be referred to as O1B, and the atom at hydrogen-bonding distance to μ^3-OH (O2B) on the zirconium cluster is designated O3. The structure was found to be identical to that reported by the previous single-crystal study[23] save for the linker occupancy, which has previously been shown to be variable and dependent on synthetic conditions.[11,21] Two notable bond lengths for this study are Zr–O1B of 2.24(3) Å and O2B–O3 of 2.730(6) Å, the latter corresponding to a hydrogen-bonding distance. The values quoted are for the optimal synthesis conditions, as discussed in the caption of Figure 2.

To investigate the nature of the defect site, the effect of sample activation in an environment cell was used to study the structure in situ in real-time under vacuum. The results are shown in Figure 4 and Table 1. A single crystal of UiO-66, synthesized using the optimal ratio of formic acid to *N*,*N*-diethylformamide (DEF), was glued to a 10 μm Kapton MiTeGen loop with a minimum amount of epoxy resin. The loop was mounted on a custom goniometer head affixed with a gas inlet and a 3 mm diameter capillary cover. The sample was then placed under vacuum overnight at room temperature (stage 1), then heated at a rate of 200 K per hour up to 500 K, where the sample was kept for 1 h (stage 2). To reduce thermal motion and obtain a more accurate structure, the sample was then cooled to 200 K (stage 3) at a rate of 360 $K\,h^{-1}$. Finally, the cell was warmed to room temperature, also at a rate of 360 $K\,h^{-1}$, and the crystal exposed to the atmosphere (stage 4).

After stage 1, structure refinement reveals the electron density at O1B is reduced compared to the as-synthesized sample, converging to 5.0 ± 1.0% of the oxygen atom O1B, and 92 ± 0.9% linker, with O1B located 2.27(6) Å from the zirconium center. From solving the structure during heating, it was found that at just above room temperature, all the

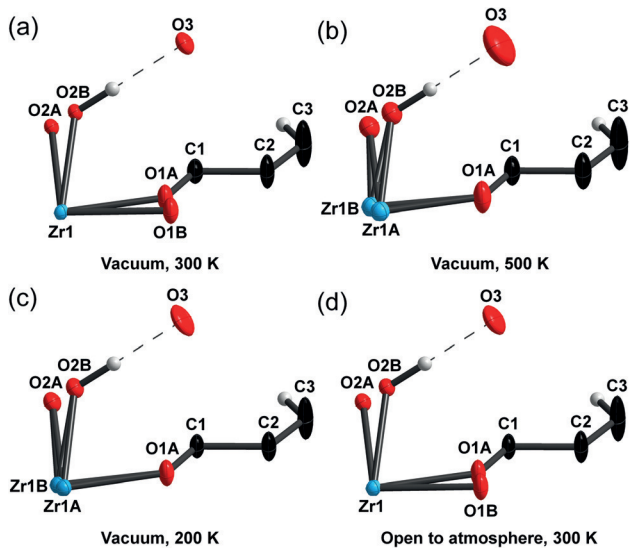

Figure 4. Asymmetric unit of UiO-66 measured in the environment cell. The measurement begins at room temperature under vacuum (a, UiO-66_GC1), then heated to 500 K at 200 K h^{-1} (b, UiO-66_GC2), during which the water molecules replacing the linker are removed to leave open metal sites on Zr. The crystal was then cooled to 200 K (c, UiO-66_GC3) for a more accurate structure determination. Finally, the crystal was warmed to room temperature and exposed to the atmosphere (d, UiO-66_GC4), where the water molecules are once again coordinated to Zr. Ellipsoids are shown at 50% probability.

Table 1: Crystallographic data for UiO-66 measured in the environment cell from stages 1 to 4.

Sample	UiO66_GC1	UiO66_GC2	UiO66_GC3	UiO66_GC4
chemical formula	$C_{44.16}H_{26.02}O_{32.18}Zr_6$	$C_{44.16}H_{26.02}O_{30.99}Zr_6$	$C_{44.16}H_{26.02}O_{30.99}Zr_6$	$C_{44.16}H_{26.02}O_{32.18}Zr_6$
formula mass	1618.87	1599.67	1599.67	1618.87
crystal system	cubic	cubic	cubic	cubic
space group	$Fm\bar{3}m$	$Fm\bar{3}m$	$Fm\bar{3}m$	$Fm\bar{3}m$
λ [Å]	0.77490	0.77490	0.77490	0.77490
a [Å]	20.7570(7)	20.7192(7)	20.7239(8)	20.7574(7)
Z	4	4	4	4
V [Å^3]	8943.2(9)	8894.4(9)	8900.5(10)	8943.7(9)
T [K]	298(2)	500(2)	200(2)	298(2)
density [g cm^{-3}]	1.202	1.195	1.194	1.202
measured reflections	8290	49181	48278	48357
unique reflections	1081	1389	1388	1396
parameters	33	32	32	33
restraints	0	0	0	0
R_{int}	0.0496	0.0328	0.0355	0.0305
θ range (deg)	2.14-39.48	2.14-43.92	2.14-43.91	2.14-43.90
R_1, wR_2	0.0357, 0.1454	0.0302, 0.1183	0.0312, 0.1191	0.0300, 0.1243
S (GOF)	1.302	1.266	1.252	1.202
max/min res. dens. [e Å^{-3}]	0.89/−0.87	01.04/−0.84	1.14/−0.82	1.34/−0.96

electron density of O1B is removed, while an oxygen atom with an occupancy of 11.3% is modeled at O3, located at 2.85(2) Å from O2B.

Stage 2 still shows no density at O1B, but intriguingly, there is still 18.2 ± 1.8% of an oxygen atom refined, fixed to 11.3% to match charge balancing, at position O3 that is at a distance of 2.83(2) Å from O2B. This suggests the hydrogen-bonded species present here are strongly bound to the metal cluster. As a confirmation, the structure at stage 3 does not change at lower temperature except that the thermal ellipsoids shrink, as expected. The relatively short hydrogen-bonding O2B−O3 distance of 2.787(15) Å combined with the consistent observation of electron density at this position, even at high temperature, strongly indicate the presence of anions.

This is also necessary considering that the negative charge lost from the missing BDC must be accounted for. The oxo and hydroxy O2A and O2B occupancies converge to 50.7 ± 0.5% and 49.3 ± 0.5%, respectively, so another species must counterbalance the charge. This can be achieved by O3 if this species is anionic, further corroborating these findings.

The only other structural change at this point is brought about by the loss of the water molecule, which produces a coordinatively unsaturated site at the zirconium center. This results in a shift of the affected zirconium ions towards the center of the metal oxide cluster, so now zirconium is disordered over two positions. This is not surprising as the coordination number is reduced while maintaining the Zr^{4+} charge, thus meaning zirconium binds more tightly to the remaining atoms in the coordination sphere.

Upon warming the crystal to room temperature and exposure to the atmosphere at stage 4, the density at O1B returns and the zirconium atom is no longer disordered, as is expected when O1B is coordinated. The bond length is 2.21(3) Å, very close to the as-synthesized sample. Since the source of O1B at this stage is from the atmosphere, this must be either water or hydroxide originating from deprotonated atmospheric water. A search through the Cambridge Structural Database consistently puts Zr−OH_2 distances around 2.2 Å, while Zr−OH is approximately 2.0 Å for an eight-coordinated zirconium center. This matches the evidence at stage 3 that anions are responsible for charge-balancing the structure, not at the defect site itself. Indeed, we postulate the defects arise from the strong hydrogen-bonding interactions of these counterions to the metal cluster, which are likely present during the synthesis based on the structure of $ZrOCl_2$ containing counterions, since the negatively charged BDC linker must substitute these anions to coordinate to the structure for charge-balancing reasons. This may be a result of an ion mobility issue once the framework begins to crystallize, thereby preventing hydroxide from replacing water bound to the zirconium ion. Similarly, the lack of space in the crystallized structure would prevent the BDC linker from coordinating.

Confirmation of the presence of anions at the positions of O3 came from the synthesis of UiO-66 starting from zirconium(IV) propoxide; a propoxide counterion is cleanly refined within hydrogen-bonding distance to the metal cluster (Figure 5a). Propoxide is still present after activation at 423 K

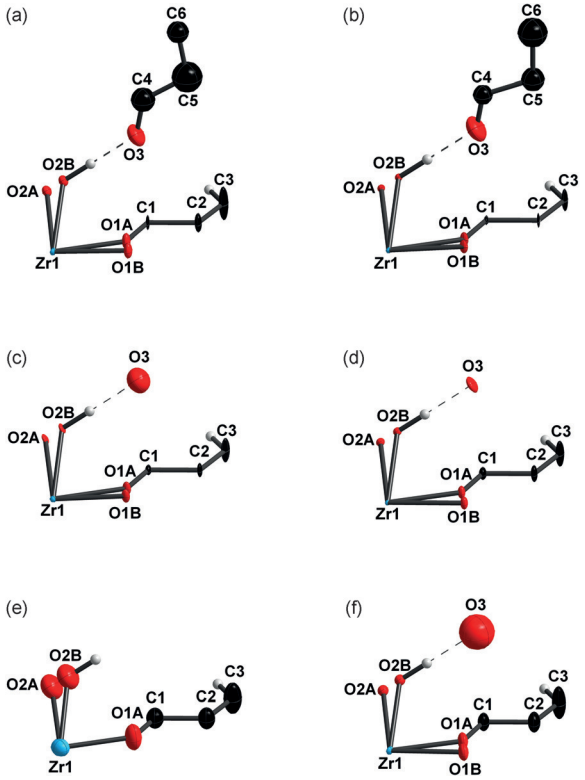

Figure 5. The asymmetric unit of UiO-66 of the as-synthesized propoxide (a) shows propoxide anions hydrogen-bonded to the cluster. This propoxide anion is not removed upon evacuation at 423 K for 24 h (b), but is removed under vacuum at 573 K for 24 h (c). Both (b) and (c) were exposed to the atmosphere after heating. Structure (d) is as-synthesized from $ZrOCl_2$ for comparison with the air-free structure of UiO-66, (e), also synthesized from $ZrOCl_2$, but evacuated at 573 K for 24 h. In (e) the hydroxide anion has been removed and the adjacent μ^3-hydroxy groups are deprotonated, thereby converting some portion to μ^3-oxo groups to achieve charge balance. Finally, (f) is the rehydrated sample after exposure to the atmosphere following activation at 573 K.

under vacuum (Figure 5b), thus suggesting it is strongly bound and charge-balances the cluster. Propoxide is favored in this position over hydroxide presumably because the former is in excess and a slightly stronger base than hydroxide, which is present in trace amounts. However, activation at 573 K successfully removes the propoxide ion, and after exposure to the atmosphere the crystal structure is indistinguishable from UiO-66 synthesized from zirconium oxychloride (Figure 5c). Indeed, the entirely air-free crystal structure of UiO-66 synthesized from the zirconium oxychloride salt after activation at 573 K reveals the loss of the counterion. As confirmation of the propoxide structure, refinements using the propoxide model were performed against the reflection data for compounds prepared from other starting salts as well as the sample activation at 573 K, which failed to converge. This treatment at 573 K corresponds to the "dehydroxylated" structure of UiO-66, previously reported as containing inorganic clusters of Zr_6O_6.[21] The results from our study indicate this conversion is partial; based on the percentage of μ^3-oxo groups we demonstrate that the μ^3-hydroxy groups adjacent to counterions transfer a proton to O3, which is expelled as water. From occupancy refinement, charge balancing is now achieved from $60.0 \pm 3.7\%$ μ^3-oxo and $39.0 \pm 3.7\%$ μ^3-hydroxy groups bound to the zirconium cluster (Figure 5e). Interestingly, upon exposure to water the structure reverts to $50.4 \pm 1.8\%$ oxo, $49.6 \pm 1.8\%$ hydroxy, and charge-balancing is achieved by the return of a counterion (Figure 5f). This agrees with the previous observation of structural reversibility from neutron powder refinement.[21] Since this process occurs upon simple exposure to the atmosphere, we postulate moisture is sufficient to protonate some of the μ^3-oxo groups to form μ^3-hydroxy groups, thereby leaving the charge-balancing hydroxide ions in the pore and hydrogen bonded to the clusters.

In syntheses starting from halide salts such as $ZrCl_4$, the anion identity of the as-synthesized samples required further investigation: no density beyond O3 can be modeled that makes reasonable chemical sense, which suggests O3 is either hydroxide or chloride. There are reports of UiO-66 containing various amounts of chloride, thus indicating the species present may be dependent on synthesis conditions.[11,23,27] Elemental analysis of the samples in this investigation reveal an average of 0.6% chlorine present after solvent exchange followed by activation of UiO-66 at 423 K. With an error of 0.3% in both accuracy and precision, this amount of chloride cannot be considered significant. With a defect percentage of 10% and no further density in the pores, 2.6% chloride by weight would be expected.

As another test for chloride, silver nitrate was added to the digested supernatant of UiO-66, but no immediate precipitation was observed. After leaving overnight, a dark brown solid formed, which is likely due to silver oxide formation.

The anion identity was further investigated by the synthesis of UiO-66 from zirconium(IV) bromide with a trace amount of added water. If bromide were hydrogen bonding to the cluster, a large increase in electron density and a longer hydrogen-bond length would be expected. SXRD reveals comparable electron density in the as-synthesized samples, with an oxo/hydroxy occupancy of $50.1 \pm 1.2\%$ compared to $49.9 \pm 1.2\%$, and a hydrogen-bond length of 2.718(18) Å, thus indicating bromide ions are not present in that position. It was also found that saturating the solution with alkali halide salts such as NaCl, KCl, NaBr, and KBr did not result in a significant increase in the electron density or number of defects.

Another possibility is that the counterions are formates because of the large amount incorporated during the synthesis. However, ^{1}H NMR digestion of UiO-66 shows there is no formate present, and it is not possible to model density beyond O3. Evidence in support of hydroxide counterions is that the hydrogen-bonding distance in the as-synthesized sample is very similar to that of the rehydrated "dehydroxy-

lated" sample. Since this species can only come from the atmosphere in the rehydrated sample, O3 must be hydroxide originating from deprotonated atmospheric water. Bringing the evidence together strongly indicates that the identity of O3 is a hydroxide ion (Figure 6).

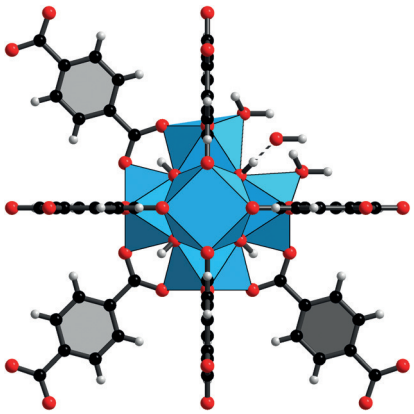

Figure 6. View of one metal cluster with a defect site where BDC is replaced by water, with the resulting loss in charge counterbalanced by a hydroxide anion.

Coupled thermogravimetric and mass spectrometric analysis shows three steps during the decomposition of UiO-66 under an argon atmosphere. The first step, beginning around 323 K confirms the loss of water molecules from the defect position. The second step at 573–723 K reveals the loss of the hydroxide counterion as water, which corresponds to the dehydroxylation step. The final step at 723–923 K is due to the decomposition of the BDC linker, with loss of CO_2 and aromatic species. No HCl gas was found to be released during this decomposition process, as would be expected if chloride was present as the counterion.

Scanning electron microscopy images show well-defined single crystals that show no apparent surface defects (Figure 7). Additionally energy-dispersive X-ray spectroscopy showed no amount of chloride, even in the samples with the highest number of defects.

In summary, we have definitively identified the linker defect sites to be occupied by water, with charge neutrality maintained by hydroxide anions hydrogen bonding to the μ^3-OH groups of the metal cluster, in the well-known and important crystal structure of UiO-66. This is a rare study in the field of solid-state chemistry and MOFs in which defects were successfully identified with molecular level precision. This study opens up the possibility to study point defects in other similar porous systems such as UiO-67, and to design in situ studies following the cluster growth formations to confirm the hypotheses put forward on defect formation.

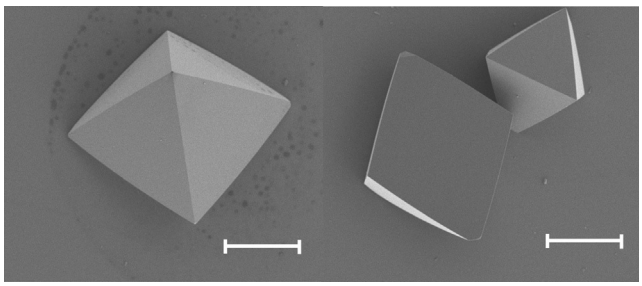

Figure 7. Scanning electron microscopy images of a single crystal of UiO-66, showing no apparent signs of a defective structure. Scale bar 100 μm.

Experimental Section

A new synthesis was developed for making large single crystals of UiO-66. It uses a combination of *N*,*N*-diethylformamide (DEF) and formic acid. A ratio of 1:1 by volume produces the largest crystals (Figure 2). The starting materials of $ZrOCl_2 \cdot 8H_2O$ (0.037 mmol) and H_2BDC (0.03 mmol) were dissolved in DEF prior to mixing and addition of formic acid. The resulting solution was placed in an oven for 2 days at 408 K. Furthermore, it was found that these conditions could be extended to a variety of zirconium salts and functionalized linkers. This includes $ZrCl_4$, $ZrBr_4$, $Zr(OPr)_4$, H_2BDC-Br, H_2BDC-NH_2, H_2BDC-NO_2, and H_2BDC-Me_2, thus demonstrating the versatility of these synthetic conditions (see the Supporting Information for further details).

Supporting information for this article is available online. CCDC 1405735–1405752, and 1406507 contain the supplementary crystallographic data for this paper. These data can be obtained free of charge from The Cambridge Crystallographic Data Centre.

Acknowledgements

This work, including synthesis, characterization, and crystal structure analysis was funded by BASF SE (Ludwigshafen, Germany) and the U.S. Department of Defense, Defense Threat Reduction Agency (HDTRA 1-12-1-0053). Work performed at the Advanced Light Source is supported by the Director, Office of Science, Office of Basic Energy Sciences, of the U.S. Department of Energy under Contract No. DE-AC02–05CH11231. We acknowledge Y. Zhao (Yaghi group) for his assistance with electron microscopy; Dr. P. Siman (Yaghi group) for discussions; and Dr. S. Teat for the synchrotron X-ray diffraction data acquisition support at the beamline 11.3.1 (Advanced Light Source, Lawrence Berkeley National Laboratory). F.G. acknowledges the Spanish Ministry of Economy and Competitiveness for funding through the Juan de la Cierva program.

Keywords: metal-organic frameworks · single crystals · structure elucidation · UiO-66 · X-ray diffraction

How to cite: *Angew. Chem. Int. Ed.* **2015**, *54*, 11162–11167
Angew. Chem. **2015**, *127*, 11314–11319

[1] J. D. Jorgensen, D. G. Hinks, P. G. Radaelli, S. Pei, P. Lightfoot, B. Dabrowski, C. U. Segre, B. A. Hunter, *Phys. C* **1991**, *185–189*, 184–189.
[2] A. R. West, *Basic Solid State Chemistry*, Wiley, Weinheim, **1999**.
[3] R. Long, N. J. English, O. V. Prezhdo, *J. Am. Chem. Soc.* **2013**, *135*, 18892–18900.
[4] B. Murugan, A. V. Ramaswamy, *J. Am. Chem. Soc.* **2007**, *129*, 3062–3063.

[5] J. K. Nørskov, T. Bligaard, B. Hvolbaek, F. Abild-Pedersen, I. Chorkendorff, C. H. Christensen, *Chem. Soc. Rev.* **2008**, *37*, 2163 – 2171.
[6] T. Aoki, Y. Chang, G. Badano, J. Zhao, C. Grein, S. Sivananthan, D. J. Smith, *J. Cryst. Growth* **2004**, *265*, 224 – 234.
[7] R. Ameloot, F. Vermoortele, J. Hofkens, F. C. De Schryver, D. E. De Vos, M. B. J. Roeffaers, *Angew. Chem. Int. Ed.* **2013**, *52*, 401 – 405; *Angew. Chem.* **2013**, *125*, 419 – 423.
[8] R. H. Rickman, P. R. Dunstan, *J. Raman Spectrosc.* **2014**, *45*, 15 – 21.
[9] X. Stammer, S. Heißler, *Spectroscopy* **2013**, *28*, 22 – 27.
[10] P. St. Petkov, G. N. Vayssilov, J. Liu, O. Shekhah, Y. Wang, C. Wöll, T. Heine, *ChemPhysChem* **2012**, *13*, 2025 – 2029.
[11] M. J. Cliffe, W. Wan, X. Zou, P. A. Chater, A. K. Kleppe, M. G. Tucker, H. Wilhelm, N. P. Funnell, F.-X. Coudert, A. L. Goodwin, *Nat. Commun.* **2014**, *5*, 4176 – 4183.
[12] M. Sturza, J. M. Allred, C. D. Malliakas, D. E. Bugaris, F. Han, D. Y. Chung, M. G. Kanatzidis, *Chem. Mater.* **2015**, *27*, 3280 – 3290.
[13] Y. Janssen, D. Santhanagopalan, D. Qian, M. Chi, X. Wang, C. Hoffmann, Y. S. Meng, P. G. Khalifah, *Chem. Mater.* **2013**, *25*, 4574 – 4584.
[14] Z. Fang, B. Bueken, D. E. De Vos, R. A. Fischer, *Angew. Chem. Int. Ed.* **2015**, *54*, 7234 – 7254; *Angew. Chem.* **2015**, *127*, 7340 – 7362.
[15] Z. Fang, J. P. Du, M. Kauer, W. Zhang, C. Lochenie, B. Jee, B. Albada, N. Metzler-Nolte, A. Po, B. Weber, et al., *J. Am. Chem. Soc.* **2014**, *136*, 9627 – 9636.
[16] K. J. Gagnon, H. P. Perry, A. Clearfield, *Chem. Rev.* **2012**, *112*, 1034 – 1054.
[17] B. Tu, Q. Pang, D. Wu, Y. Song, L. Weng, Q. Li, *J. Am. Chem. Soc.* **2014**, *136*, 14465 – 14471.
[18] M. Shoaee, M. W. Anderson, M. P. Attfield, *Angew. Chem. Int. Ed.* **2008**, *47*, 8525 – 8528; *Angew. Chem.* **2008**, *120*, 8653 – 8656.
[19] F. Vermoortele, R. Ameloot, L. Alaerts, R. Matthessen, B. Carlier, E. V. R. Fernandez, J. Gascon, F. Kapteijn, D. E. De Vos, *J. Mater. Chem.* **2012**, *22*, 10313 – 10321.
[20] J. H. Cavka, S. Jakobsen, U. Olsbye, N. Guillou, C. Lamberti, S. Bordiga, K. P. Lillerud, *J. Am. Chem. Soc.* **2008**, *130*, 13850 – 13851.
[21] H. Wu, Y. S. Chua, V. Krungleviciute, M. Tyagi, P. Chen, T. Yildirim, W. Zhou, *J. Am. Chem. Soc.* **2013**, *135*, 10525 – 10532.
[22] L. Valenzano, B. Civalleri, S. Chavan, S. Bordiga, M. H. Nilsen, S. Jakobsen, K. P. Lillerud, C. Lamberti, *Chem. Mater.* **2011**, *23*, 1700 – 1718.
[23] S. Øien, D. Wragg, H. Reinsch, S. Svelle, S. Bordiga, C. Lamberti, K. P. Lillerud, *Cryst. Growth Des.* **2014**, *14*, 5370 – 5372.
[24] H. Wu, T. Yildirim, W. Zhou, *J. Phys. Chem. Lett.* **2013**, *4*, 925 – 930.
[25] F. Vermoortele, B. Bueken, G. Le Bars, B. Van de Voorde, M. Vandichel, K. Houthoofd, A. Vimont, M. Daturi, M. Waroquier, V. Van Speybroeck, et al., *J. Am. Chem. Soc.* **2013**, *135*, 11465 – 11468.
[26] M. J. Katz, Z. J. Brown, Y. J. Colón, P. W. Siu, K. A. Scheidt, R. Q. Snurr, J. T. Hupp, O. K. Farha, *Chem. Commun.* **2013**, *49*, 9449 – 9451.
[27] G. C. Shearer, S. Chavan, J. Ethiraj, J. G. Vitillo, S. Svelle, U. Olsbye, C. Lamberti, S. Bordiga, K. P. Lillerud, *Chem. Mater.* **2014**, *26*, 4068 – 4071.
[28] A. Clearfield, P. A. Vaughan, *Acta Crystallogr.* **1956**, *9*, 555 – 558.

Received: June 14, 2015
Published online: August 7, 2015

